

EVALUATION OF PERI-TUMORAL VESSELS SURROUNDING COLORECTAL LIVER METASTASES AFTER INTRAVENOUS INJECTION OF EXTRUDED MAGNETOLIPOSOMES IN RATS: CORRELATION WITH 3T MRI AND HISTOPATHOLOGY

K. Coenegrachts¹, J. van Werven², L. ter Beek³, Z. Mzallassi⁴, M. Bögels⁵, Th. van Gulik⁴, I. Van Den Berghe⁶, A. Nederveen², J. Stoker², H. Rigauts¹, S. Soenen⁷, M. De Cuyper⁷

Background: Magnetoliposomes have pronounced signal-enhancing effect on T1-weighted (T1w) images of the liver using qualitative analysis which may be beneficial for demonstrating peritumoral vasculature.

Purpose: To correlate peri-tumoral vasculature (ring-enhancement) surrounding colorectal liver metastases after injection of magnetoliposomes using T1-weighted (T1w) imaging with histopathology in a rat model.

Material and Methods: All experiments were approved by the responsible Animal Care Committee. Three rats injected with CC531 coloncarcinoma cells in the portal vein were imaged at 3T using a small diameter four channel coil. The presence of liver metastases, signal intensity changes within intrahepatic vessels, peri-tumoral vasculature (ring-enhancement) surrounding liver metastases on T1w imaging and histopathology, and the histopathological distribution of iron particles were evaluated. SS SE-EPI and T1w GE sequences were used. Images were evaluated qualitatively and MRI findings were correlated with histopathology.

Results: Fifteen liver metastases were present which were all detected at MRI (mean diameter 2.4 mm (SD 0.8 mm, range 1.5 -4.7 mm)). Ring-enhancement surrounding liver metastases at contrast-enhanced T1w GE sequences was present in all liver metastases. Correlation with histopathology showed the corresponding presence of dilated sinusoids filled with iron particles surrounding the liver metastases.

Conclusion: Blood-pooling of iron oxide particles within magnetoliposomes was demonstrated with increased and hyperintensity of vessels after injection of magnetoliposomes. Qualitatively, ring-enhancement surrounding the liver metastases was seen on T1w imaging and corresponded histopathologically with the presence of iron particles (magnetoliposomes) within the dilated sinusoids surrounding the liver metastases.

Key-words: Liver neoplasms, secondary – Neoplasms, blood supply.

The early detection and therapy of liver metastases is of utmost importance in patients with cancer. Colorectal cancer is a frequent malignancy and is one of a few malignant tumors in which the presence of limited synchronous liver metastases (i.e. occurring at the time of diagnosis of the primary tumor) or metachronous metastases (occurring after diagnosis of the primary tumor) warrants surgical resection (1). Exact knowledge of the number, size, and regional distribution of liver metastases is essential to determine their resectability. To provide this information, radiologists have used computed tomography (CT) – with best results during arteriography (2, 3) – and superparamagnetic iron oxide (SPIO)-enhanced magnetic res-

onance imaging (MRI) (4-6). SPIO-enhanced MRI has high sensitivity that matches that of CT during arteriography and higher specificity than that of CT during arteriography (5, 6). The primary advantage of SPIO-enhanced MRI is that, unlike CT during arteriography, it is noninvasive. SPIO-enhanced MRI is now regarded by many physicians as the best available examination technique in the evaluation of liver metastases (7).

SPIO-particles were originally developed as contrast medium for MRI of the liver, where they are administered to improve tumor detection at T2-weighted imaging. Intravenously injected SPIO particles also shorten the T1 relaxation time. The T1-shortening effect is particular-

ly improved for ultras-small SPIO (USPIO) particles (8-11). For the characterization of malignant focal liver lesions ring-enhancement has already been described as a potential useful sign and optimized demonstration of this enhancement is therefore advantageous (12). In this regard also the blood-pool effect of (U)SPIO particles can be useful. Extruded magnetoliposomes can be fine-tuned so that a higher ratio of T1 shortening to T2 shortening is achieved. Thus, on the basis of these observations, we hypothesized that extruded magnetoliposomes with only a few USPIO grains in their aqueous cavity may generate a pronounced signal-enhancing effect on T1-weighted (T1w) images of the liver.

In this pilot study, MRI experiments were performed using a rat model with CC531 colorectal liver metastases. The effect of magnetoliposomes injection for the evaluation of peri-tumoral vessels was qualitatively examined using T1w GE sequences and histopathology. This study was performed to provide a proof-of-principle for using magnetoliposomes as a useful blood-pool agent for the qualitative characterization of liver metastases using magnetoliposomes-enhanced T1w imaging.

From: 1. Department of Radiology, AZ St.-Jan Brugge-Oostende AV, Bruges, Belgium, 2. Department of Radiology, Academic Medical Center, Amsterdam, The Netherlands, 3. Philips Healthcare, Eindhoven, The Netherlands, 4. Department of Surgery/Surgical Laboratory, Academic Medical Center, Amsterdam, The Netherlands, 5. Department of Molecular Cell biology and Immunology, VU University Medical Center, Amsterdam, The Netherlands, 6. Department of Pathology, AZ St.-Jan Brugge-Oostende AV, Bruges, Belgium, 7. Interdisciplinary Research Center, Catholic University Leuven-Campus Kortrijk, Kortrijk, Belgium

Address for correspondence: Dr K. Coenegrachts, M.D., Ph.D., Department of Radiology, AZ St.-Jan Brugge-Oostende AV, Ruddershove 10, B-8000 Bruges, Belgium
E-mail: kenneth.coenegrachts@azbrugge.be

Material and methods

During previous experiments performing MRI on tubes filled with different concentrations of magnetoliposomes r1 and r2 values were calculated. These values allowed an optimization of the MRI sequences and allowed determining an optimal concentration of iron particles within the magnetoliposome's interior space (see appendix).

All animal experiments were approved by the responsible Animal Care Committee. Three rats injected with CC531 coloncarcinoma cells in the portal vein were imaged at 3T.

Animals and procedures

Three male Wag/Rij rats (Harlan, Horst, The Netherlands) weighting 250–270g were acclimatized for one week under standardized laboratory conditions in a temperature-controlled room with 12-h dark/light cycles. Animals were given free access to water and standard chow (Hope Farms, Woerden, The Netherlands). Especially the evaluation of micrometastases (< 10 mm) are important from a clinical point of view. In this pilot study, liver metastases ranging from 1–10 mm are included for this purpose.

The following sequence in manipulations was applied:

1. On day 0 all rats underwent median laparotomy with anesthesia as follows:

Isoflurane (Florene, Abbott Laboratories, Queensborough, United Kingdom) anesthesia was used. The rats were placed in an anesthesia chamber and exposed to a gas mixture of 0.3 L/min oxygen, 0.6 L/min air and 2–4% isoflurane (total percentage of oxygen of about 40%). When the rat was completely relaxed it was removed from the chamber and exposed to a gas mixture of 0.75 L/min oxygen, 1.5 L/min nitrous oxide and 2–2.5% isoflurane (total percentage of oxygen of about 40%). By means of a pain stimulus the rat was checked for accurate narcosis. During narcosis the rat was placed on a warming blanket to avoid cooling down.

Then, all rats were injected with a dose of 200.000 CC531 coloncarcinoma cells in the portal vein for the induction of colorectal liver metastases. These CC531 coloncarcinoma cells had been in culture for 10 days. The abdomen was closed in two layers using a running 4-0 vicryl suture (Ethicon) and the animals were allowed to wake up.

2. At day 10 and subsequently on day 15 (as no liver metastases were seen on day 10) two rats were controlled for the presence of liver metastases prior to the injection of magnetoliposomes by using laparoscopic inspection. Isoflurane (Florene, Abbott Laboratories, Queensborough, United Kingdom) anesthesia was used for scopic evaluation. These two rats underwent a scopic evaluation (Karl Storz Endoscopy-America Inc., Culver City, California, United States of America) via an abdominal incision of 1 centimeter at day 10 post injection of the CC531 coloncarcinoma cells. This same scopic evaluation was repeated on day 15 as no liver metastases were detected during the first scopic evaluation. The abdomen was closed in two layers using a running 4-0 vicryl suture (Ethicon) and the animals were allowed to wake up.

3. Just before the start of the MRI experiment, all rats were anesthetized with intraperitoneal injection of FFM (0.27 ml/100 gr weight: 1 ml Hypnorm (VetaPharma Ltd, Leeds, United Kingdom), 1 ml Dormicum (Roche bv, Woerden, The Netherlands), 2 ml water (B. Braun, Meisungen, Germany)) and subsequently anesthetized by inhalation of a mixture of O₂/air (1:1 v/v, 2 L/min) containing 2–2.5% isoflurane (Florene, Abbott Laboratories, Queensborough, United Kingdom). Then the rats underwent the MRI experiment.

Contrast media and doses

The magnetoliposomes used here were of the extruded type (13, 14). They consist of large unilamellar vesicles with a diameter of around 100 nm, capturing Fe₃O₄ nanocores (diameter ~ 2 nm). In practice, a mixture of dimyristoylphosphatidylcholine, dimyristoylphosphatidylglycerol and the distearoylphosphatidylethanolamine~poly(ethylene glycol)₂₀₀₀ adduct (molar ratio 85/10/5) was incubated with citrate-coated Fe₃O₄ particles having a diameter of about 2 nm (15) and subsequently extruded at room temperature through two polycarbonate filters of 0.1 µm pore size. Non-encapsulated magnetic particles were removed by ion-exchange chromatography (type EMD-TMAE). The final contrast agent solution contained 0.073 mmol phospholipid and 7.88 µg Fe₃O₄ per ml. Based on these values it was calculated that each individual magnetoliposome structure contained approximately 7 magnetite cores.

In all three rats, 0.75 ml of magnetoliposomes were injected in a tail vein immediately followed by 0.5 ml of saline. Both injections were performed by hand injection.

MRI imaging protocol

All MRI experiments were performed using the 4-channel wrist coil on 3T MRI (Achieva, Philips Medical Systems, Best, The Netherlands). The rats were placed in the head coil in the supine position. At the start of the MRI protocol, a survey and reference scan were performed. Then a SS SE-EPI sequence and a fat-suppressed T1w 3D GE sequence were used before injection of magnetoliposomes. Immediately after intravenous manual bolus injection of 0.8 cc of magnetoliposomes followed by 0.5 ml of saline via the tail vein, the T1w GE sequence was performed in the arterial and venous phases (FS T1w GE sequence performed at start of injection, 1 minute, 3, 5, 10 and 15 minutes after intravenous injection of magnetoliposomes).

The BB SE SE-EPI sequence was applied with following parameters: TR: 1200 ms, TE: 50ms, flip angle: 90°, scan plane: axial, NSA (Number of Signal Averages indicates the number of times each (acquired) line in k-space is sampled): 4, FOV (Field-of-View): 65 mm x 65 mm, scan percentage (is a percentage of phase-encoding values (profiles) of k-space around k = 0 profile): 100%, half scan factor (is a method in which approximately only one half of k-space in the phase-encoding direction is acquired): 1, Act.BW (actual band width): 29,4, ST (slice thickness): 4 mm, SPAIR (SPectral Attenuated Inversion Recovery) TR: 240 ms.

The T1w 3D GE sequence was applied with following parameters: TR: 6 ms, TE: 2,9 ms, flip angle: 10°, scan plane: axial, NSA: 4, FOV: 120 mm x 120 mm, scan percentage: 100%, half scan factor: 1, Act.BW: 289,4, ST (slice thickness): 2 mm, SPAIR TR: 181,2 ms.

Sacrifice of the rats and histopathological analysis

Immediately after the MRI experiment, the animals were sacrificed during anesthesia and bled to death after resection of the liver.

Then all livers were removed for histopathological examination and fixed in 10% buffered formalin for 1 week. All the livers were sliced and macroscopically examined by a

pathologist having 25 years of experience. All metastatic tumors were located and the largest tumor diameter was measured. Histological sections were made from all metastatic lesions and the surrounding parenchyma. The sections were stained with hematoxylin and eosin and a pearls iron stain.

Analysis of the MRI findings with histopathological findings

A visual (qualitative) analysis of the SS SE-EPI and T1w GE sequences was performed by an experienced abdominal radiologist (9 years of experience in abdominal MRI).

The SS SE-EPI sequence was evaluated for the detection of liver metastases and compared with the (unenhanced and all contrast-enhanced) T1w GE sequences concerning liver metastasis detection. The liver metastases detected upon applying the various MRI sequences were correlated with histopathology. The T1w GE sequences were also evaluated for contrast-enhancement of the intrahepatic vessels and for the detection of ring-enhancement surrounding the liver metastases. The T1w GE sequences were correlated with the histopathological findings to evaluate the potential of magnetoliposomes-enhanced T1w GE imaging in characterizing liver metastases. Further the histopathological distribution of the iron particles was evaluated.

Statistical analysis

For this pilot study only descriptive data presentation was possible.

Results

The different metastatic lesions showed typical histopathological findings of an adenocarcinoma. In the surrounding liver parenchyma, an accentuated component of blue staining iron was seen on the pearls stain. Histopathology did not detect any additional liver metastases which were not detected by the applied MRI sequences.

Compared with T1w GE, the SS SE-EPI sequence detected the maximum number of liver metastases in all three rats. No additional liver metastases were detected using the T1w sequences. Unenhanced T1w GE sequences had too low contrast-to-noise ratio for appropriate evaluation of the liver metastases. In rat 1, rat 2 and rat 3 respectively 8, 5 and 2 liver metastases were detected

using the applied MRI sequences. SS SE-EPI detected 3 respectively 2 additional liver metastases in rat 1 respectively rat 2 compared with the T1w sequences. The diameter of the detected liver metastases using MRI ranged from 1.5 mm to 4.7 mm (mean: 2.4 mm ; SD: 0.8 mm). All liver metastases detected on MRI were confirmed by histopathology. Visual (qualitative) evaluation of the MRI examinations showed the appearance of hyperintense signal within the hepatic vessels after injection of magnetoliposomes with persisting hyperintense signal using the delayed contrast-enhanced T1w sequences. Liver metastases were better visualized as hypo-intense lesions using contrast-enhanced T1w sequences compared with unenhanced T1w sequence. Ring-enhancement surrounding liver metastases was present in all detected liver metastases using contrast-enhanced T1w GE sequences (Fig. 1). Correlation with histopathology (Fig. 1) showed the corresponding presence of dilated sinusoids filled with iron particles surrounding the liver metastases. Neo-angiogenic vessels within the liver metastases were not visualized by histopathological examination.

Discussion

In this study CC531 colon carcinoma cells were used for our rat model as these cells show comparable growth characteristics with human colon carcinoma cells. The results of this study show that magnetoliposomes-enhanced T1w GE sequences can visualize ring-enhancement at the periphery of the liver metastases. Ring-enhancement on T1w imaging corresponded with the presence of iron particles (blood-pooling of magnetoliposomes) within the dilated sinusoids surrounding the liver metastases on histopathology. Ring-enhancement on T1w sequences was useful for the detection and characterization of liver metastases in this study. Unenhanced SS SE-EPI was the most accurate MRI sequence for the detection of (the smallest) liver metastases.

In the literature, a commercially available hepato-specific contrast agent containing SPIO (ferucarbotran (Resovist®)) has already been used for the characterization of colorectal liver metastases (8, 16-18). It appeared that dynamic T1w scanning with ferucarbotran significantly improves the differentiation of

benign and malignant focal liver lesions compared with unenhanced MRI and T2w MRI pre/post-ferucarbotran alone. Clinical studies with dynamic T1w GE demonstrated the presence of ring-enhancement surrounding liver metastases. This effect has been explained by neovascularity and blood-pool effects of vessels surrounding malignant focal liver lesions (12, 19).

To further improve the T1-effect of the iron-oxide particles in this study, we used smaller iron-oxide particles encapsulated within PEGylated magnetoliposomes to avoid phagocytosis and to allow blood-pooling. In this study, the injection of magnetoliposomes in combination with T1w imaging allowed the characterization of colorectal liver metastases by demonstrating typical ring-enhancement surrounding the liver metastases.

The persistent hyperintensity on T1w GE of the vessels can be explained by the PEGylation of the magnetoliposomes ("stealth-magnetoliposomes") leading to increased blood-pooling. Using a blood-pool agent was considered important for this study as the purpose was to evaluate peri-tumoral vessels. Therefore, migration of the magnetoliposomes from the intravascular space to the interstitial space was inhibited.

To our knowledge the use of stealth magnetoliposomes using magnetoliposomes-enhanced T1w imaging for the detection and characterization (demonstration of blood-pooling and ring-enhancement surrounding liver metastases) of liver metastases has not been evaluated before.

The MRI protocol used in this study consisted of MRI sequences that are already used in clinical practice. In this pilot study CC531 colon carcinoma cells were used for our rat model as these cells show comparable growth characteristics with human colon carcinoma cells. This will allow easier extrapolation of our results for future use of the MRI experiments in oncological patients.

From table 1 (see appendix) we can see that the ratio of the relaxivities $r1/r2$ at 3.0T is substantially higher for the magnetoliposomes than for Resovist®. This means that the magnetoliposomes used in this work have a stronger T1 effect relative to T2 compared to Resovist®. It is also shown that the $r1/r2$ ratio decreases with increasing field strength. Therefore one should be careful to use the commonly cited

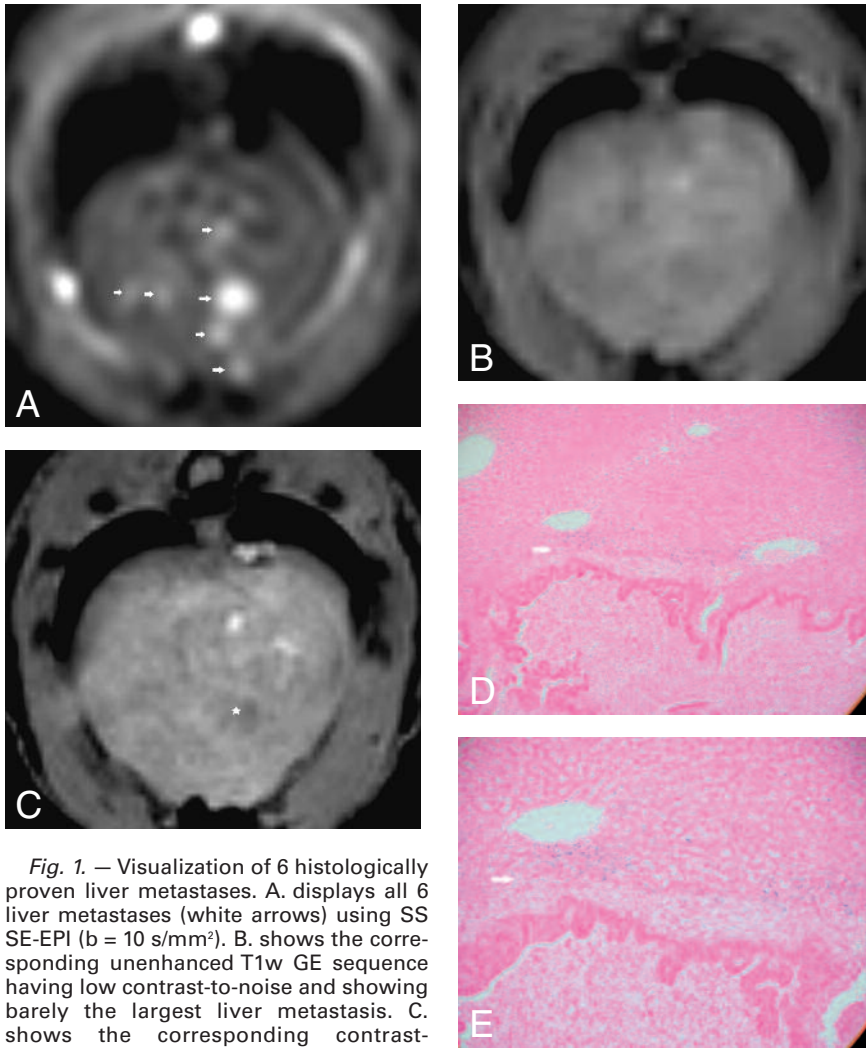


Fig. 1. — Visualization of 6 histologically proven liver metastases. A. displays all 6 liver metastases (white arrows) using SS SE-EPI ($b = 10 \text{ s/mm}^2$). B. shows the corresponding unenhanced T1w GE sequence having low contrast-to-noise and showing barely the largest liver metastasis. C. shows the corresponding contrast-enhanced T1w GE sequence (1 minute post ML injection) showing the largest liver metastasis (white star) with surrounding ring-enhancement. D. shows the corresponding histological image at the level of the largest liver metastasis. Blue iron stain was used. In the lower part a close-up of the liver metastasis is shown. Dilated sinusoids with iron particles (magnetoliposomes; blue particles in the image) are seen surrounding the liver metastasis (magnification factor 20x). The periphery of the liver metastasis is located at the level of the white arrow. E. shows the corresponding histological image at the level of the largest liver metastasis. Blue iron stain was used. In the lower part a detail of the liver metastasis is shown. Dilated sinusoids with iron particles (magnetoliposomes; blue particles in the image) are seen surrounding the liver metastasis (magnification factor 200x). The periphery of the liver metastasis is located at the level of the white arrow.

values of r_1 and r_2 at 0.47T, since most clinical scanners operate at 1.5T and 3.0T. It should be noted, however, that there is a possible error due to potential nonlinear concentration dependencies of the relaxation rates for these large magnetoliposomes. The solvent was distilled water and no proteins were present like in the case of blood plasma. Proteins may have an effect on the relaxation rates due to possible binding to the contrast agents and increasing the viscosity of the solvent.

Visual/qualitative evaluation of (small) focal liver lesions can be dif-

ficult in differentiating true-positive focal liver lesions from false-positive focal liver lesions. Paging through the stack of MRI slices facilitates this task. Further, the visual identification of all the detected lesions was also correlated with other sequences (SS SE-EPI sequence and contrast-enhanced T1w sequences). This allowed to differentiate focal liver lesions from intrahepatic vessels. The calculation of lesion-to-liver contrast-to-noise ratio can help in this differentiation although these calculations are less accurate (volume-averaging effect) in small focal liver lesions. Therefore, in this pilot

study only visual/qualitative evaluation (with paging through the MRI images) was used.

The persisting ring-enhancement after injection of (blood-pool/stealth) magnetoliposomes supported the characterization of malignant liver lesions (liver metastases). The rather low resolution of the MRI images in this study and the small diameter of the liver metastases in this study made the evaluation of the ring-enhancement more difficult. Paging through the stack of images allowed to better appreciate the ring-enhancement surrounding the liver metastases.

In this study no magnetoliposomes could be detected within the neo-angiogenic vessels of the liver metastases. This might be caused by the rather small calibre of the studied liver metastases in this study. Further, the use of a pure (100%) blood-pool agent might not be optimal for the detection of these small neo-angiogenic vessels. For the detection of neo-angiogenesis, it might be interesting to evaluate other magnetoliposomes with different size having blood-pool characteristics but with selective leakage only through neo-angiogenic vessels. This might allow an indirect measurement of the amount of neo-angiogenic vessels.

In conclusion, the T1-effect and blood-pooling of the iron oxide particles within the magnetoliposomes is demonstrated with increased hyperintensity of vessels after injection of magnetoliposomes. Ring-enhancement surrounding the liver metastases is seen using qualitative evaluation of T1w imaging and is caused by the presence of iron particles within the dilated sinusoids surrounding the liver metastases. Further research is needed to optimize these magnetoliposomes and to allow transport of magnetoliposomes to (and through) the neo-angiogenic vessels within the liver metastases.

References

- Schima W., Kulinna C., Langenberger H., Ba-Ssalamah A.: Liver metastases of colorectal cancer: US, CT or MR? *Cancer Imaging*, 2005, 5: S149-S155.
- Soyer P., Levesque M., Caudron C., Elias D., Zeitoun G., Roche A.: MRI of liver metastases from colorectal cancer vs CT during arterial portography. *J Comput Assist Tomogr*, 1993, 17: 67-74.
- Schmidt J., Strotzer M., Fraunhofer S., Boedeker H.,

Zirngibl H.: Intraoperative ultrasonography versus helical computed tomography and computed tomography with arteriography in diagnosing colorectal liver metastases: lesion-by-lesion analysis. *World J Surg*, 2000, 24: 43-47.

4. Seneterre E., Taourel P., Bouvier Y., et al.: Detection of hepatic metastases: ferumoxides-enhanced MR imaging versus unenhanced MR imaging and CT during arterial portography. *Radiology*, 1996, 200: 785-792.
5. Vogl T.J., Schwarz W., Blume S., et al.: Preoperative evaluation of malignant liver tumors: comparison of unenhanced and SPIO (Resovist)-enhanced MR imaging with biphasic CTAP and intraoperative US. *Eur Radiol*, 2003, 13: 262-272.
6. Strotzer M., Gmeinwieser J., Schmidt J., et al.: Diagnosis of liver metastasis from colorectal adenocarcinoma: comparison of spiral-CTAP combined with intravenous contrast-enhanced spiral-CT and SPIO-enhanced MR combined with plain MR imaging. *Acta Radiol*, 1997, 38: 986-992.
7. Nasu K., Kuroki Y., Nawano S., Kuroki S., Tsukamoto T., Yamamoto S., Motoori K., Ueda T.: Hepatic Metastases: Diffusion-weighted Sensitivity-encoding versus SPIO-enhanced MR Imaging. *Radiology*, 2006, 239: 122-130.
8. Saini S., Edelman R., Sharma P., et al.: Blood-pool MR contrast material for detection and characterization of focal hepatic lesions: initial clinical experience with ultrasmall superparamagnetic iron oxide (AMI-227). *AJR*, 1995, 164: 1147-1152.
9. Saini S., Sharma R., Baron R.L., et al.: Multicentre dose-ranging study on the efficacy of USPIO ferumoxtran-10 for liver MR imaging. *Clin Radiol*, 2000, 55: 690-695.
10. Sahani D., Saini S., Sharma R., O'Malley M., Hahn P.: Dynamic T1-weighted ferumoxides enhanced MRI for imaging liver hemangiomas: preliminary observations. *Abdom Imaging*, 2001, 26: 166-170.
11. Müller M., Reimer P., Wiedermann D., et al.: T1-weighted dynamic MRI with new superparamagnetic iron oxide particles (Resovist): results of a phantom study as well as 25 patients. *Rofo*, 1998, 168: 228-236.
12. Mergo P., Helmberger T., Nicolas A., Ros P.: Ring enhancement in ultrasmall supermagnetic iron oxide MR imaging: a potential new sign for characterization of liver lesions. *AJR*, 1996, 166: 379-384.
13. Sabaté R., Barnadas-Rodríguez R., Callejas-Fernández J., et al.: Preparation and characterization of extruded magnetoliposomes. *Int J Pharm*, 2008, 347: 156-162.
14. Soenen S.J.H., Hodenius M., De Cuyper M.: Magnetoliposomes: versatile innovative nanocolloids for use

Table I. – Relaxivity values for Resovist® and for the magnetoliposomes.

RELAXIVITY IN WATER [L*MMOL ⁻¹ *S ⁻¹]	RESOVIST®			MAGNETOLIPOSOME (3.0T)	
	ref.a (0.47T)	ref. b (0.47T)	ref. b (3.0T)	[vesicles]	[Fe3O4]
r1	24.7	20.6	4.6	1205	182
r2	163.8	86	143	1905	288
r1/r2	0.151	0.24	0.032	0.633	0.633

Legend: Ref.a: Monograph Resovist, Schering AG, 2002; Ref.b: Rohrer M., Bauer H., Mintonovitch J., Requardt M., Weinmann H.: *Invest Radiol*, 2005, 40: 715-724.

in biotechnology and biomedicine. *Nanomedicine*, 2009, 4: 177-191.

15. Hodenius M.A.J., Niendorf T., Krombach G.A., et al.: Synthesis, physicochemical characterization and MR relaxometry of aqueous ferrofluids. *J Nanoscience Nanotechnology*, 2008, 8: 2399-2409.
16. Reimer P., Jahnke N., Fiebich M., et al.: Hepatic lesion detection and characterization: value of non-enhanced MR imaging, superparamagnetic iron oxide-enhanced MR imaging, and spiral CT-ROC analysis. *Radiology*, 2000, 217: 152-158.
17. Van Gansbeke D., Metens T., Matos C., et al.: Effects of AMI-25 on liver vessels and tumors on T1-weighted turbo-field-echo images: implications for tumor characterization. *J Magn Reson Imaging*, 1997, 7: 482-489.
18. Reimer P., Müller M., Marx C., et al.: T1 effects of a bolus-injectable superparamagnetic iron oxide, SH U 555 A: dependence on field strength and plasma concentration – preliminary clinical experience with dynamic T1-weighted MR imaging. *Radiology*, 1998, 209: 831-836.
19. Harisinghani M., Saini S., Weissleder R., et al.: Differentiation of liver hemangiomas from metastases and hepatocellular carcinoma at MR imaging enhanced with blood-pool contrast agent code-7227. *Radiology*, 1997, 202: 687-691.

Appendix

Before the start of this in vivo experiment, we determined the T₁ and T₂ relaxation times of several sample tubes with a range of concentrations of magnetoliposomes. The T₁ times were determined from a standard inversion recovery sequence in a point-resolved spectroscopy sequence for a selected 1 x 1 x 1 cm³ voxel within each sample tube. The MR signal was measured as a function of inversion time

(TI) and fitted off-line to three parameters of the function which described the MR signal recovery.

$$S(TI) = A(1 - Be^{-\frac{TI}{T_1}})$$

where S(TI) is the MR signal (peak height and peak integral in the spectrum) at an inversion time TI, A is the signal at thermal equilibrium, B is a factor of 2 under perfect experimental conditions when applying a 180 degree RF pulse, and C is the T₁ relaxation time. The T₁ relaxation times were also determined by a Look-Locker MR protocol and found to be in excellent agreement with the spectroscopy results (unpublished data).

The T₂ times were determined with a point-resolved spectroscopy sequence within a 1 x 1 x 1 cm³ voxel for each sample tube. The MR signal was measured as a function of the echo-time TE and fitted off-line to three parameters of the function which describes the T₂ decay

$$S(TE) = Ae^{-\frac{TE}{T_2}} + C$$

Where S(TE) is the MR signal (peak height and peak integral of the spectrum) at echo-time TE, A is the signal at thermal equilibrium, B is the T₂ relaxation time, and C is the baseline noise level to which the signal decays.

The repetition time TR in the spectroscopy protocols was chosen sufficiently long to prevent saturation effects, usually around 10 s. Relaxivity values for Resovist® and for the magnetoliposomes used in this study are given in table 1.